

Alterations in the histaminergic system in Alzheimer's disease: a postmortem study

Ling Shan^{a,b}, Koen Bossers^b, Unga Unmehopa^b, Ai-Min Bao^{a,*}, Dick F. Swaab^b

^a Department of Neurobiology, Key Laboratory of Medical Neurobiology of Ministry of Health of China, Zhejiang Province Key Laboratory of Neurobiology, Zhejiang University School of Medicine, Hangzhou, China

^b Netherlands Institute for Neuroscience, an Institute of the Royal Netherlands Academy of Arts and Sciences, Amsterdam, the Netherlands

Received 19 July 2011; received in revised form 13 December 2011; accepted 22 December 2011

Abstract

Histamine is produced by the hypothalamic tuberomammillary nucleus (TMN). We studied its involvement in Alzheimer's disease (AD) by in situ hybridization of histidine decarboxylase (HDC), the key enzyme of histamine production, in 9 AD patients and 9 controls. Additionally, messenger (m) RNA levels of the 4 histamine receptors (H₁₋₄R) and of the enzyme involved in histamine metabolism, histamine methyltransferase (HMT), were determined by quantitative polymerase chain reaction (qPCR) in the prefrontal cortex (PFC) in the course of AD ($n = 49$). Moreover, alterations in glia markers were studied. HDC-mRNA levels in the TMN were unchanged in AD, despite of the reduced number of Nissl-stained neurons ($p = 0.001$). However, a decrease in HDC-mRNA was observed in its medial part (mTMN; $p = 0.047$). In the course of AD only females had increased prefrontal cortex expression of histamine receptor-3 (H₃R) ($p = 0.007$) and histamine methyltransferase-mRNA ($p = 0.011$) and of the glia markers, glial fibrillary acidic protein-mRNA, vimentin-mRNA and proteolipid protein-mRNA. These findings indicate the presence of regional changes in the TMN that are at least partly gender-dependent. © 2012 Elsevier Inc. All rights reserved.

Keywords: Histamine; Alzheimer's disease; Tuberomammillary nucleus; Prefrontal cortex; Histamine receptors; Histamine methyltransferase

1. Introduction

Neuronal histamine is exclusively produced in the hypothalamic tuberomammillary nucleus (TMN) by the rate-limiting enzyme L-histidine decarboxylase (HDC) (Panula et al., 1984). It is mainly degraded by histamine-N-methyltransferase (HMT) (Husztai et al. (1998)), and glia plays an important role in its inactivation (Rafałowska et al., 1987). Histaminergic fibers project to a large number of brain areas, including the cerebral cortex, thalamus, basal ganglia, amygdala, and hippocampus, where histamine is crucially involved in a large number of basic physiological functions, such as the sleep-wake cycle, energy metabolism and en-

docrine homeostasis, sensory and motor functions, cognition, attention, learning, and memory (Haas et al., 2008). All these modalities are severely affected in Alzheimer's disease (AD) (Martorana et al., 2011).

The reports on alterations in the histaminergic system in AD are equivocal. On the one hand it has been postulated that histamine production would be decreased due to an accumulation of neurofibrillary tangles (NFT) in the TMN in the early stages of the AD process (i.e., in Braak stage 3) (Braak et al. (1993)) and to a loss of large histaminergic neurons in the rostral TMN in AD (Nakamura et al., 1993). These findings are in agreement with high performance liquid chromatography results showing that histamine levels diminish in a number of brain areas in AD (Mazurkiewicz-Kwilecki and Nsonwah, 1989; Panula et al., 1998) and with the decreased neuronal metabolic activity of the TMN observed in AD (Nakamura et al., 1993; Salehi et al., 1995). Moreover, a positron emission tomography study showed that in AD patients, histamine receptor-1 (H₁R) binding was

* Corresponding author at: Department of Neurobiology, Key Laboratory of Medical Neurobiology of Ministry of Health of China, Zhejiang Province Key Laboratory of Neurobiology, Zhejiang University School of Medicine, Hangzhou, China. Tel: +86 571 88208789; fax: +86 571 88208248.

E-mail address: baoaimin@zju.edu.cn (A.-M. Bao).

decreased in the frontal and temporal cortex (Yanai and Tashiro, 2007). However, several other reports claim that the histaminergic system may be hyperactive both in healthy aging subjects (Prell et al., 1988) and in AD patients (Cacabelos et al., 1989; Fernández-Novoa and Cacabelos, 2001). In AD patients, increased histamine levels were found not only in the frontal cortex, basal ganglia, and hippocampus (Cacabelos et al., 1989), but also, together with its metabolites, in the cerebrospinal fluid (CSF) (Fernández-Novoa and Cacabelos, 2001). It should be noted that differences in putative confounding factors, such as postmortem delay (PMD), gender, and age may have contributed to the variable results (Panula et al., 1998). Moreover, special attention should be paid to possible sex differences in studies of the histaminergic system, because more cytoplasmic estrogen receptor (ER)- α staining was found in the TMN of men than of women (Kruijver et al., 2002), while, in addition, the CSF concentration of histamine metabolites in women tended to be higher than in men (Motawaj et al., 2010; Prell et al., 1990). Furthermore, the densities of H₁R and histamine receptor-2 (H₂R) were found to be higher in the female than in the male rat cortex (Ghi et al., 1999).

The aim of the present study was to determine, for the first time, the possible alterations of neuronal histamine production in AD by relating the changes of TMN neuron numbers to histamine production as determined by quantitative in situ hybridization of HDC-messenger (m) RNA expression in the TMN in the last stage of AD (Braak 6) (Braak and Braak, 1991). In addition, in 1 of the major neuronal histamine projection areas, the prefrontal cortex (PFC), we used real time quantitative polymerase chain reaction (qPCR) to assess the mRNA levels of the 4 major histamine receptors (HRs) (H₁₋₄R) and of HMT, as well as of several glia markers: glial fibrillary acidic protein (GFAP) and vimentin (VIM) as astrocyte markers (Eng et al., 2000; Jing et al., 2007; Pekny and Pekna, 2004), proteolipid protein (PLP) as oligodendrocyte marker (Duncan et al., 1987; Lees et al., 1984), and differentiation molecule 11 β (CD11b) as microglia marker (Koning et al., 2007) in each stage of AD (Braak stage 0–6). These markers were determined because the glial cell is presumed to play an important role in histamine inactivation (Husztai et al., 1998). Furthermore, double-labeling of HMT-mRNA in situ hybridization and GFAP-immunocytochemistry was performed to explore the localization of histamine inactivation in the human PFC.

2. Methods

2.1. Postmortem brain material

Formalin-fixed, paraffin-embedded hypothalami (9 AD patients of Braak stage 6, and 9 control subjects of Braak stage 0/1) (Braak and Braak, 1991) and snap-frozen medial frontal gyrus tissue (7 subjects per Braak stage, thus in total

49 subjects from Braak 0 to Braak 6; for details see Bossers et al., 2010) were obtained through the Netherlands Brain Bank (NBB) and matched for sex, age, clock time and month of death, and PMD (for clinicopathological information, see Tables 1 and 2). The diagnosis of AD and establishing of the patients' Braak stage and the control status, were confirmed by systematic neuropathological analyses as described before (van de Nes et al., 1998). Written informed consent for the brain autopsy and the use of the brain material and medical records for research purposes was acquired by the NBB from patients or their next of kin. Exclusion criteria for control subjects were primary neurological and/or psychiatric disorders. In addition, any AD patient or control subject treated with histamine receptor (reverse) agonists was excluded.

The hypothalami were serially sectioned at 6 μ m intervals along the rostrocaudal axis. Every 100th section was Nissl stained by thionin to determine the borders of the TMN. The frozen PFC tissue samples have been extensively described in our previous studies (Bossers et al., 2010; Luchetti et al., 2011). Briefly, based on the distribution of neurofibrillary tangles (Braak and Braak, 1991), 7 patients were chosen for each Braak stage (Braak 1–6) and 7 subjects without tangles (Braak 0). Subsequently, 3 subgroups were made based upon the cognitive characteristics of the Braak stages: Braak 0–2, no cognitive impairment; Braak 3–4, mild cognitive impairment; and Braak 5–6, fully developed AD (Baner et al., 1996). It should be noted, however, that although this subdivision was made on the basis of studies comparing the relationship between the neuropathological Braak-AD stages and the clinical states for groups of patients (Dubelaar et al., 2006), there can be quite some variability in this relationship on an individual level.

RNA extracted from the frozen tissue was of high integrity, i.e., RNA integrity number (RIN): mean 8.3, range 6.5–9.6, which is well within the quality requirements for qPCR analysis (Fleige and Pfaffl, 2006).

2.2. TMN neuron counts

In order to localize the TMN, a Nissl staining by thionin was performed on every 100th section along the rostrocaudal axis throughout the hypothalamus. Based upon the thionin staining, the TMN borders were roughly defined as the distance between the most rostral and the most caudal section that contained 3 or more typical TMN neurons (Swaab, 2003), while the borders were subsequently determined more precisely by in situ hybridization for HDC-mRNA (see below) for which also 1 in every 100 sections was used. Following thionin staining, the total number of neurons was estimated at 600 μ m intervals throughout the TMN. In each section, all TMN neurons with their typical cell profiles and a visible nucleolus serving as a unique marker for each neuron, were counted using light microscopy at a magnification \times 400. Taking into account the interval distances

Table 1

Clinicopathological details of subjects used for TMN cell counts and HDC mRNA measurements

	NBB	Sex	Age (y)	CTD	MOD	BW (g)	FT (d)	Braak stage	ApoE	PMD	Cause of death
Controls	1998-027*	M	54	9:00	12	1350	59	0	ND	8:00	Respiratory insufficiency secondary to severe bronch-pneumonia and sepsis
	1999-116*	M	78	16:45	9	1300	43	0	33	6:15	Pancreatic cancer
	1995-106*	M	74	13:00	11	1317	60	0	32	5:45	Myocardial infarction
	1995-093*	M	78	4:00	9	1440	29	1	33	20:00	Decompensatio cordis, fever as a result of pulmonary embolism
	1998-081	M	63	7:40	4	1368	65	1	ND	8:00	Severely extended double-sided pneumonia causing ventricular tachycardia
	1997-156*	F	77	8:30	11	1235	47	1	ND	4:20	Septic shock; metastasized pancreas carcinoma
	1998-036*	F	69	9:25	3	1229	31	1	33	8:00	Cardiogenic shock
	2001-069*	F	68	12:15	5	1135	32	1	43	7:00	Euthanasia
	1998-035	F	65	21:00	1		55	0	ND	1:40	Complications with mesenterial ischemia
	Mean	5 M/4 F	69.6			1296.7	46.8			7:37	
	SEM		2.7			33.7	4.6			1:54	
	Median		69				47			6:37	
	Percentile										
	25th		64				31.5			4:41	
AD			77.5				59.5			8:00	
	1996-020	M	58	5:20	2	1180	27	6	33	5:50	Cachexia
	2000-066	M	80	18:35	6	1160	31	6	43	3:50	Dehydration and vascular insufficiency
	2001-136	M	73	15:40	12	1176	47	6	32	3:45	Sepsis
	2002-082	M	72	11:50	9	1181	39	6	42	3:35	Broncho-pneumonia complicated by slight cardiac decompensation
	2003-107	M	69	21:05	12	1013	31	6	ND	5:10	Pneumonia caused by aspiration and cardiac decompensation
	2004-023	F	67	17:45	3	1135	40	6	42	4:20	Cachexia
	2003-057	F	68	4:30	6	985	41	6	32	6:35	Pneumonia/dehydration
	2000-140	F	72	18:50	12	980	31	6	43	5:30	Dehydration
	1996-109	F	66	12:40	10	1020	120	6	33	8:00	Marasmus seniles due to dementia
	Mean	5 M/4 F	69.4			1092.2	45.2			5:10	
	SEM		2			9.6	30			0:29	
	Median		69			1135	39			5:10	
	Percentile										
	25th		66.5			999	31			3:47	
			72.5			1178	44			6:12	
	<i>p</i> value	1	0.894			0.001	0.258			0.423	

Braak stage for Alzheimer's disease (AD): progression of pathological changes in AD was according to Braak et al., 1993. *p* value: differences between 2 groups were tested using the Mann-Whitney *U* test.

Key: ApoE, apolipoprotein E; BW, brain weight; CTD, clock time at death; F, female; FT, fixation time in days; HDC, histidine decarboxylase; M, male; mRNA, messenger RNA; MOD, month of death; NBB, Netherlands Brain Bank number; ND, no data; PMD, postmortem delay; SEM, standard error of the mean; TMN, tuberomamillary nucleus.

Table 2

Clinicopathological information of frozen prefrontal cortex samples used for qPCR

Braak stage (<i>n</i> = 7 per group)	Age (y)	Sex	PMD (h)	CSF pH	RIN
0	70.6 ± 3.6	4 M/3 F	6.8 ± 0.6	6.7 ± 0.2	8.1 ± 0.4
1	80.3 ± 2.1	3 M/4 F	6.0 ± 0.4	6.6 ± 0.1	8.7 ± 0.4
2	76.7 ± 3.0	3 M/4 F	7.3 ± 0.6	6.7 ± 0.1	9.1 ± 0.0
3	85.0 ± 2.4	3 M/4 F	6.0 ± 0.9	6.7 ± 0.1	7.7 ± 0.3
4	82.3 ± 1.9	3 M/4 F	5.1 ± 0.6	6.6 ± 0.1	8.2 ± 0.3
5	74.3 ± 2.5	4 M/3 F	5.6 ± 0.5	6.5 ± 0.1	8.3 ± 0.3
6	70.3 ± 3.0	3 M/4 F	4.7 ± 0.3	6.8 ± 0.1	7.6 ± 0.2
<i>p</i> Value	0.004	0.992	0.042	0.468	0.043

Braak stage for Alzheimer's disease (AD): progression of pathological changes in AD according to Braak et al., 1993. *p* Value: differences between 7 groups were tested by Kruskal-Wallis. Values are presented as mean ± standard error of the mean.

Key: CSF, cerebrospinal fluid; F, female; M, male; PMD, postmortem delay; qPCR, quantitative polymerase chain reaction; RIN, RNA integrity number.

between individual sections the total number of TMN neurons was determined based on the Cavalieri principle described before (Verwer and Raber-Durlacher, 1993). We further subdivided the rostral-caudal length of the TMN into 3 equal parts, thus distinguishing in 3 subregions: a rostral (rTMN), medial (mTMN), and caudal (cTMN) part. These subdivisions were similar to a previously performed arbitrary subdivision (Nakamura et al., 1993).

2.3. Quantitative radioactive HDC-mRNA *in situ* hybridization in the TMN

Quantitative *in situ* hybridization (ISH) was performed according to the protocol that we developed and have described in detail before (Liu et al., 2010). For the assessment of HDC-mRNA in the TMN, we used a 45-mer oligonucleotide antisense probe (GenBank # NM_002112: 5' GGC AGG ACT CAT CAG CAT CGG GCT CAG ACG TTT TCA TTT CCA GGA 3') targeted to bases 647–603 of the human HDC-mRNA sequence. An HDC sense probe (5' TCC TGG AAA TGA AAA CGT CTG AGC CCG ATG CTG ATG AGT CCT GCC 3') was used to serve as a negative control. In brief, the probe was 3'-end labeled with ³⁵S-dATP (PerkinElmer Life and Analytical Sciences, Waltham, MA, USA; Catalog no. NEG734H) using terminal deoxynucleotidyl transferase (Roche Diagnostics, Basel, Switzerland). The labeled probe was purified through ethanol precipitation and suspended in a hybridization buffer (HBF: 0.5 M NaCl, 1× Denhardt's solution, 10 mM Tris-HCl, 1 mM ethylenediaminetetraacetic acid [EDTA], 10% dextran sulfate, 0.5 mg/mL yeast tRNA, 50% formamide, 800 mM dithiothreitol [DTT]). Every 100th section (6 μm) along the rostrocaudal axis of the TMN was deparaffinized in xylene and rehydrated via a descending series of ethanol, then autoclaved for 20 minutes at 120 °C under a pressure of 1 bar in 0.01 M citrate buffer (pH 6.0). Following delipidation in phosphate buffered saline (PBS; 0.15 M NaCl, 9 mM Na₂HPO₄, 1.7 mM NaH₂PO₄) containing 0.1% Triton X-100, sections were hybridized in HBF containing approximately 1 × 10⁶ cpm of labeled HDC oligoprobe per slide. The hybridization took place overnight in a humidi-

fied box in a stove at 42 °C. The next day, sections were washed sequentially for 30 minutes at 46 °C in 1 × standard saline citrate (SSC), 2 × 15 minutes at 46 °C in 0.1 × SSC, 2 × 15 minutes at room temperature in 0.1 × SSC, and were dehydrated in 300 mM ammonium acetate (pH 5.5)/absolute ethanol mixtures at volume ratios of 1:1, 3:7, 1:9, and 0:1, respectively. Sections were then exposed to autoradiographic film for 2 weeks, after which the films were developed for 3–4 minutes in Kodak D-19 developer (Eastman Kodak Company, Rochester, NY, USA) and fixed in Kodak Maxfix (Eastman Kodak Company) for 5 minutes.

Gray values of individual autoradiograms of TMN sections were related to an existing standard curve. The outcome was multiplied by the area covered by the HDC signal to obtain an estimate for the total amount of HDC-mRNA in the TMN, expressed in arbitrary units (AU). For details, see Liu et al., 2010.

2.4. qPCR study in the frozen PFC tissue

Details of dissection of the gray matter from the snap-frozen postmortem PFC tissue, subsequent RNA isolation and cDNA synthesis are described in our previous studies (Bossers et al., 2010; Luchetti et al., 2011). The qPCR procedures have also been described in detail previously (Luchetti et al., 2011). In brief, it was performed in a reaction volume of 20 μL, using the SYBR Green PCR Kit (Applied Biosystems, Warrington, UK) and a mixture of sense and antisense primers (2 pmol/μL). For detailed primer information please see Supplementary Table 1. Reactions were run in a GeneAmp 7300 thermocycler under the following conditions: 2 minutes at 50 °C and 10 minutes at 95 °C, followed by 40 cycles of 15 seconds at 95 °C and finally 1 minute at 60 °C. Data were acquired and processed automatically by the Applied Biosystems Sequence Detection Software v1.4. Specificity of amplification was checked by means of melting curve analysis and electrophoresis of products on an 8% polyacrylamide gel. Sterile water (non-template control) and omission of reverse transcriptase (non-RT control) during cDNA synthesis served as negative controls. Amplification efficiency was determined by run-

ning qPCR reactions on a dilution series of pooled cDNA from all the subjects. The resulting cycle threshold (Ct) values were plotted against the inverse log of each dilution and the slope of this curve was then used to calculate the efficiency as follows: efficiency (E) = $10^{-1/\text{slope}}$. The normalization factor was based upon the geometric mean of the following 7 reference genes selected by geNorm analysis (Vandesompele et al., 2002), i.e., *AURKAIP1*; *DHX16*; *ERBPPLHDC5*; *ISOC2*; *SNW1*; and *TM9SF4*. The relative absolute amount of target genes was calculated with the use of the following formula: $10^{10} \times E^{-Ct}$. The relative mRNA expression of the target gene was obtained by dividing the calculated absolute amount of transcript by the normalization factor.

2.5. HMT-mRNA in situ hybridization followed by immunocytochemical staining of GFAP

Because HMT-mRNA levels were found to be positively correlated with GFAP-mRNA both in controls and AD patients (see Results 3.3.1.), HMT-mRNA in situ hybridization and GFAP immunocytochemistry were performed on formalin-fixed paraffin-embedded 6- μ m sections of PFC from the same subjects in order to define the detailed location of HMT-mRNA. One PFC section per subject was used.

2.5.1. In situ hybridization for HMT-mRNA in the PFC tissue

For detection of HMT-mRNA we performed in situ hybridization using a locked nucleic acid (l) and 2'-O-methyl-RNA (m) modified oligonucleotide, 5'-labeled with fluorescein (FAM5') (Ribotask, Odense, Denmark). This probe was complementary to base pair 179–197 of the human HMT-mRNA sequence (Genbank NM_001024074.2: FAM5'-lTmUmClCmCmAIGmUmUICmCmCITmCmUITmUmCIT-3'). As a negative control we used an HMT mRNA sense probe (FAM5'-lAmGmAIAmAmGIAmGmGIAmGmAICmUmGIGmGmAIA-3'). The specificity of HMT-mRNA was performed based upon the PFC tissue of 1 control (NBB # 01-004) and 1 AD subject (NBB # 98-147).

Sections of PFC were collected and mounted on Super frost plus slides (Merck, Darmstadt, Germany) using a water bath set at 48 °C. After mounting they were dried over 2 nights in a stove at 37 °C. The sections were deparaffinized in xylene for 10 minutes, then cleared for another 10 minutes in fresh xylene. Subsequently, the tissue was rehydrated in a graded ethanol series (2 \times 5 minutes in 100% ethanol, 1 minute in each 96%, 80%, and 60% ethanol) and washed twice for 2 minutes in PBS. Sections were washed for 5 minutes in 0.01 M citrate buffer pH 6.0 and subsequently microwaved in 0.1 M citrate buffer pH 6.0 for 2 \times 5 minutes at full power (700 W). Sections were allowed to cool down to room temperature for 30 minutes. Then they were washed in PBS for 2 \times 5 minutes and deproteinized as follows: the sections were incubated in 0.2 N HCl for 20 minutes, washed twice in PBS for 5 minutes and deprotein-

ated for 15 minutes in a solution containing proteinase K (Invitrogen, Carlsbad, CA, USA) (5 μ g/mL) in 1 \times prot K buffer (2 mM CaCl₂, 10 mM Tris/HCl, pH 7.5). To stop the reaction, the sections were incubated for 30 seconds in glycine buffer (26.6 mM glycine in PBS) and washed 2 \times 5 minutes in PBS. Lipids were removed from the tissue by incubating for 10 minutes in PBS-Triton (PBS containing 0.1% vol/vol Triton X-100; Sigma, Steinheim, Germany) and subsequent rinsing 2 \times 5 minutes in PBS. Sections were prehybridized in 200 μ L HBF overnight covered with Nescofilm (Bando Chemical IND, Kobe, Japan) at room temperature in a humidified chamber. The next day the probe was diluted in HBF to a final concentration of 50 nM, denatured at 95 °C for 5 minutes, and cooled on ice. Sections were hybridized in hybridization mix at 57 °C for 90 minutes, washed for 5 minutes in 5 \times SSC at 57 °C, 5 minutes in 2 \times SSC at 57 °C, 5 minutes 0.2 \times SSC at 57 °C, and 5 minutes in PBS at room temperature, and preincubated with Tris-buffered saline (TBS)-milk (1% nonfat dry milk; Elk, Campina, Woerden, the Netherlands) in TBS, pH 7.6, for 1 hour at room temperature, followed by a 3-hour incubation with sheep immunoglobulin G (IgG), antifluorescein-Fab fragments coupled to alkaline phosphatase 1:3000 (Roche, Mannheim, Germany) in Supermix-milk (SUMI-milk: 0.25% gelatin; Merck) (wt/vol), 0.5% Triton X-100 (vol/vol) in TBS-milk, pH 7.6. Next, the slides were washed 2 \times 5 minutes with 0.1 M Tris, 150 mM NaCl buffer pH 7.5, then after a prewash in 100 mM Tris-HCl pH 9.5, 100 mM NaCl, 5 mM MgCl₂, the sections were developed in NBT (Sigma), BCIP (Roche) coloring solution (337.5 μ g/mL nitro blue tetrazolium chloride, 175.4 μ g/mL 5-bromo-4-chloro-3-indolyl phosphate, toluidine salt, 240 μ g mL⁻¹ levamisole in 100 mM Tris-HCl pH 9.5, 100 mM NaCl, 5 mM MgCl₂) for approximately 25 minutes at room temperature under dark conditions. Sections were then washed in aqua dest, rinsed in 100% methanol (Sigma) for 5 minutes and washed again in aqua dest. Finally, the sections were coverslipped with Mowiol (10% wt/vol Mowiol 4–88; Calbiochem, Merck, Darmstadt, Germany,) in 0.1 M Tris-HCl pH 8.5, 25% vol/vol glycerol) aqueous mounting medium and stored in a light box at 4 °C.

2.5.2. Followed immunocytochemical staining of GFAP

Sections that were double-labeled for HMT-mRNA and GFAP were first hybridized in situ as described above for HMT-mRNA and subsequently immunocytochemically stained for GFAP. After the in situ hybridization procedure, sections were processed as follows: following methanol treatment and rinsing in aqua dest, sections were washed in TBS for 2 \times 5 minutes. Subsequently, sections were preincubated in TBS-1.25% milk (wt/vol, Elk, Campina) for 45 minutes at room temperature and then incubated in rabbit IgG against pan-GFAP (Dako, Glostrup, Denmark) at 1:1000 dilution in Supermix (Merck)-2.5% (wt/vol) milk for 1 hour at room temperature, followed by an overnight incubation at 4 °C in a moist chamber. The next day,

sections were washed in TBS for 20 minutes and then incubated in biotinylated goat anti-rabbit IgG, diluted 1:400 in Supermix (Merck) for 1 hour at room temperature. After washes in TBS for 20 minutes, sections were incubated in ABC complex (Vector Laboratories, Burlingame, CA, USA) for 1 hour. After 2 washes in TBS, sections were equilibrated for 5 minutes in acetic acid buffer (29.6 mM acetic acid, 70.4 mM sodium acetate, pH 5.0) and then developed in AEC solution (0.05% wt/vol) 3-amino-9-ethylcarbazole in acetic acid buffer, 0.015% H₂O₂ for approximately 15 minutes, washed in TBS, and finally cover-slipped in Mowiol (Calbiochem).

2.6. Statistical analysis

All data are presented as median in the text and as median (25th–75th percentile) in the Figures. Percentage changes of mRNA levels or cell densities were calculated using the mean values, in order to allow comparison with previous reports. Differences between the 2 groups were tested using the Mann-Whitney *U*-test. For comparison of gene expression over the 3 AD-Braak stages, the Kruskal-Wallis test (K-W) was employed. If a significant difference was identified among the 3 stages, each combination of 2 stages was then compared by the Mann-Whitney *U* test (M-W *U*). Intergroup differences in clock time and month of death were evaluated using the Mardia-Watson test. Spearman's ρ was used for all correlations. *p*-values ≤ 0.05 were considered to be significant (2-tailed). Because the analysis of sex differences was based upon small group sizes, a power analysis was employed to calculate the minimum effect size, using 80% as standard of adequacy (PASS 6.0, NCSS Inc., UT, USA). Statistical analyses were carried out using SPSS Statistics 17.0 (SPSS, Inc., Chicago, IL, USA).

3. Results

3.1. Possible confounders

In the study on the TMN, there was no significant difference regarding sex, age, PMD, and fixation time between the groups ($p \geq 0.258$) (Table 1) and there was no significant correlation between these putative confounding factors with either HDC-mRNA expression levels or TMN neuron numbers ($p \geq 0.306$).

In the qPCR study, due to the stringent clinical selection criteria, the final set of samples contained small differences in the Braak stages for age, PMD, and RIN value (Kruskal-Wallis test, p -value < 0.05 , Table 2). However, these differences did not confound the qPCR results, either in our previous experiments (Bossers et al., 2010; Luchetti et al., 2011) or in the present study, because age, PMD, and RIN had no correlation with the expression data of the 4 receptors and HMT in a Spearman test ($p \geq 0.119$). No significant correlation was found between duration of AD and the levels of gene expression ($p \geq 0.107$) in AD subjects.

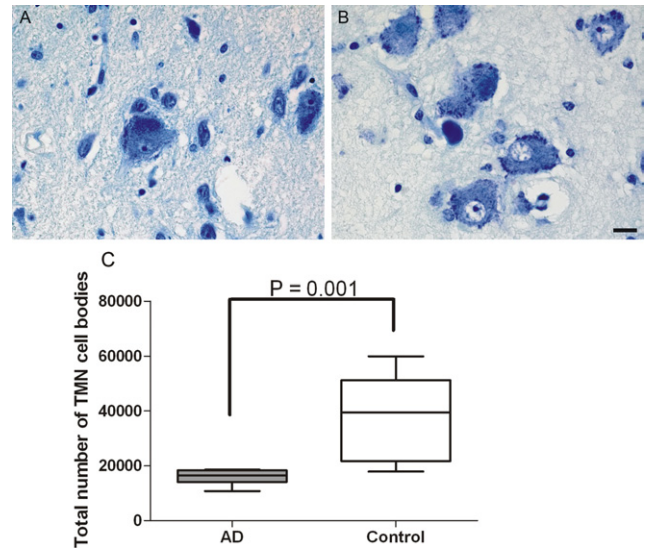


Fig. 1. Representative photographs of tuberomammillary nucleus (TMN) neurons in the posterior hypothalamus following Nissl staining of a Braak stage 6 Alzheimer's disease (AD) subject (A, Netherlands Brain Bank [NBB] # 03107) and a control (B, NBB# 98035). The pictures were taken at the level with the highest numbers of TMN neurons. Note the severe loss of the characteristic large-sized TMN neurons. Scale bar represents 0.05 mm (C). Box plot showing the median, 25th–75th percentiles, and the range of the number of TMN neurons in AD patients and controls. The total number of TMN neurons is significantly (57%) decreased compared with matched controls (Mann-Whitney *U* test: $n = 9$, $p = 0.001$).

3.2. TMN

The total number of typical TMN neurons was significantly (57%) reduced in AD patients (median = 16,436) compared with matched controls (median = 39,441) ($p = 0.001$) (Fig. 1). In contrast, HDCmRNA expression in the entire TMN in AD (median 57.4) was not significantly different from that in controls (median 108.0) ($p = 0.310$; Table 3, Fig. 2). In addition, a significant reduction in the number of neurons was found in AD patients in all 3 TMN subregions (rTMN $p = 0.009$; mTMN $p = 0.002$; cTMN $p = 0.047$, respectively) (Fig. 3A), while a significantly lower HDC mRNA expression was only found in the mTMN ($p = 0.047$), but not in the rTMN ($p = 0.566$) or in the cTMN ($p = 0.691$) (Fig. 3B).

3.3. PFC

The Kruskal-Wallis test showed that there were, in the course of AD, significant differences for levels of histamine receptor-3 (H₃R) (K-W $p = 0.003$) and HMT-mRNA (K-W $p = 0.009$) over the 3 AD-Braak-stage subgroups. Histamine receptor-4 (H₄R)-mRNA showed a trend toward a significant difference among the subgroups (K-W $p = 0.076$), while H₁R (K-W $p = 0.527$) and H₂R mRNA levels (K-W $p = 0.901$) did not show any differences.

In the end stages of AD (Braak stages 5–6) significant increases of H₃R ($p = 0.002$) (Fig. 4A) and HMT mRNA ($p = 0.006$) (Fig. 4D) were found as compared with the

Table 3
Differences between 2 groups as tested by Mann-Whitney *U* test

Group	<i>n</i>	Number TMN neurons, median (percentiles 25th–75th)	HDC mRNA, median (percentiles 25th–75th)
AD	9	16,436 (14,112–18,301)	57.4 (47.9–111.9)
Control	9	39,441 (21,729–51,137)	108.0 (57.4–141.8)
<i>p</i>		0.001 ↓**	0.31
Male			
AD	5	17,518 (13,471–18,561)	57.4 (47.9–109.1)
Control	5	26,693 (18,381–44,916)	73.4 (26.0–121.0)
<i>p</i>		0.028 ↓*	0.917
Female			
AD	4	15,663 (13,723–17,647)	73.4 (17.8–151.9)
Control	4	47,840 (29,386–57,912)	141.8 (99.4–166.8)
<i>p</i>		0.021 ↓*	0.248

Key: AD, Alzheimer's disease; HDC, histidine decarboxylase; mRNA, ; TMN, tuberomammillary nucleus.

* $p < 0.05$, Mann-Whitney *U* test.

** $p < 0.01$, Mann-Whitney *U* test.

controls (Braak stage 0–2). In addition, HMT mRNA was significantly upregulated in preclinical AD (Braak stage 3–4) compared with the controls (Braak stage 0–2, $p = 0.022$) (Fig. 4D). Moreover, although a highly significant positive correlation between the H₃R and HMT mRNA levels on the one hand and Braak stages on the other were observed in the pooled subjects ($n = 49$, $\rho = 0.415$, $p = 0.003$, and $\rho = 0.413$, $p = 0.003$, respectively), this correlation appeared to hold only for females, not for males (see below, Result 3.4.1.).

3.3.1. Glia markers in PFC

Alterations were observed in the PFC for the astrocyte markers GFAP (K-W $p = 0.002$), VIM (K-W $p = 0.016$), and oligodendrocyte marker PLP mRNA (K-W $p = 0.013$), but not for the microglia marker differentiation molecule 11 β (K-W $p = 0.824$). The end stages of AD (Braak stage 5–6) showed a significant increase in GFAP ($p < 0.0001$; Fig. 5A), VIM ($p = 0.006$; Fig. 5D), and PLP mRNA ($p = 0.003$; Fig. 5G) compared with controls (Braak stage 0–2). Furthermore, GFAP mRNA and PLP mRNA were higher in preclinical AD (Braak stage 3–4) compared with the controls (Braak stage 0–2, $p = 0.054$, and $p = 0.043$, respectively) (Figs. 5A and D).

Positive correlations were consistently observed between GFAP mRNA and VIM mRNA in controls ($n = 21$, $\rho = 0.686$, $p = 0.001$), preclinical AD (Braak stage 3–4) ($n = 14$, $\rho = 0.846$, $p < 0.001$), and AD (Braak stage 5–6) ($n = 14$, $\rho = 0.789$, $p = 0.001$).

HMT mRNA was positively correlated with GFAP mRNA and VIM mRNA in controls ($n = 21$, $\rho = 0.673$, $p = 0.001$ and $\rho = 0.449$, $p = 0.041$, respectively) and AD ($n = 14$, $\rho = 0.635$, $p = 0.015$ and $\rho = 0.675$, $p = 0.008$, respectively), but not in preclinical AD ($n = 14$, $\rho = 0.143$, $p = 0.626$ and $\rho = -0.108$, $p = 0.714$, respectively). Only in AD did HMT mRNA correlate positively with PLP mRNA ($n = 14$, $\rho = 0.574$, $p = 0.032$).

3.3.2. HMT mRNA in situ hybridization in the PFC

The specificity of HMT mRNA in situ hybridization was supported by the distinct localization of HMT mRNA (blue staining) in neurons and GFAP staining (red) in astrocytes in the PFC (Fig. 6A). In addition, it was supported by the failure of the sense probe to show a blue signal, while the red GFAP staining was present (Fig. 6B). Higher intensity of the HMT mRNA signals was observed in the deep laminar of the PFC.

3.3.3. No colocalization of HMT mRNA and GFAP in the PFC

GFAP staining was homogeneously localized across the PFC and absent in neurons (Fig. 6A–D). The HMT mRNA (blue) labeling was only observed in neurons, and there were no colocalizations of HMT mRNA and GFAP in the PFC.

3.4. Sex differences in the TMN

In controls, the total number of TMN neurons was slightly (32%), but not significantly ($p = 0.142$) higher in females ($n = 4$, median = 47,840) than in males ($n = 5$, median = 26,693) (Table 3), while HDC mRNA expression showed significantly higher (46%) levels in females than in males ($p = 0.050$; power analysis 99.4%) (Table 3). Despite relatively low numbers of the samples, the power level remained adequate (>80%) for analysis.

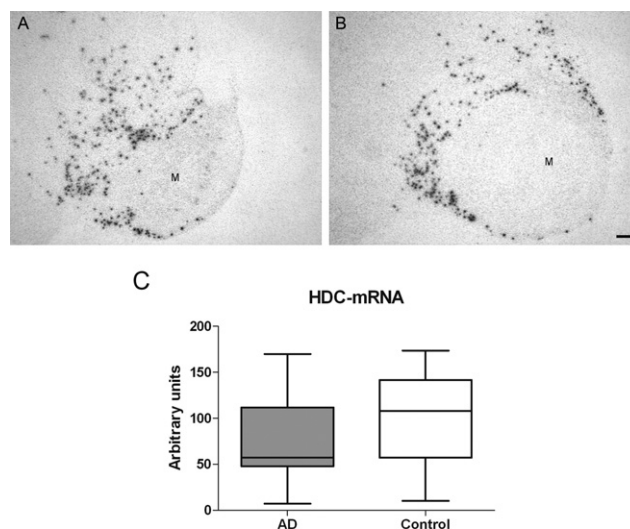


Fig. 2. Film autoradiograms of representative sections of a Braak stage 6 Alzheimer's disease (AD) patients (A, Netherlands Brain Bank [NBB] # 00140) and control (B, NBB # 01069) showing the positive tuberomammillary nucleus (TMN) neurons surrounding the negative mamillary body (M). Bar represents 1 mm. (C) Box plot showing the median, 25th–75th percentiles, and the range of the total histidine decarboxylase (HDC) messenger RNA expression in the TMN of AD patients and controls. The total amount of HDC mRNA expression was unchanged in AD patients (Mann-Whitney *U* test: $n = 9$, $p = 0.310$).

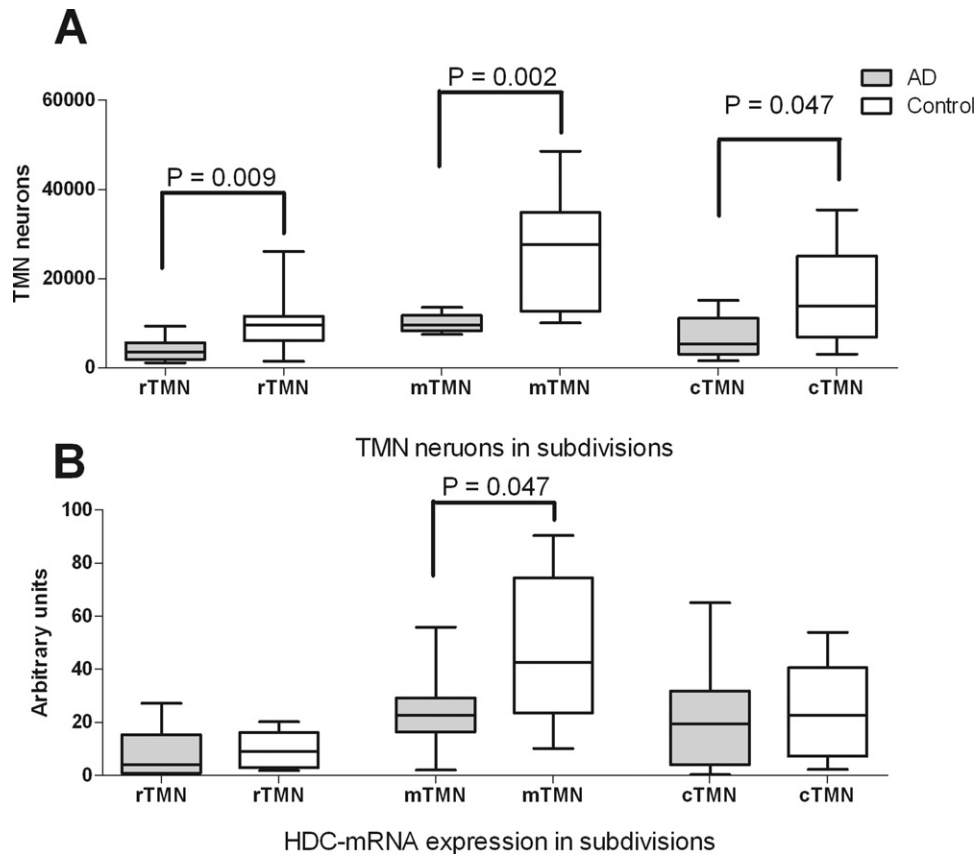


Fig. 3. Boxplot showing the median, 25th–75th percentiles, and the range of the tuberomammillary nucleus (TMN) neurons (A) and histidine decarboxylase (HDC) messenger (m) RNA expression (B) in the 3 parts of TMN area of Braak stage 6 Alzheimer's disease (AD) patients and controls. Note that the total number of TMN neurons is significantly diminished in all subregions. The HDC mRNA expression was reduced only in mTMN; p value is from Mann-Whitney U test; $n = 9$ in each box plot. Abbreviations: cTMN, caudal part of TMN; mTMN, medial part of TMN; rTMN, rostral part of TMN.

In AD patients, no sex differences were observed, either in the total amount of TMN neurons ($p = 0.462$) or in total HDC mRNA expression ($p = 0.806$) (Table 3).

3.4.1. Sex differences in the PFC

Only in females were H_3R (K-W $p = 0.007$), HMT (K-W $p = 0.011$), GFAP (K-W $p = 0.007$), VIM (K-W $p = 0.023$), and PLP (K-W $p = 0.02$) mRNA expression levels found to be significantly increased over the 3 AD-Braak subgroups. In contrast, in male subjects H_3R (K-W $p = 0.312$), HMT (K-W $p = 0.607$), GFAP (K-W $p = 0.116$), VIM (K-W $p = 0.204$), and PLP (K-W $p = 0.369$) mRNA expression was unchanged in the 3 AD-Braak subgroups. In addition, an upregulation of H_3R ($p = 0.002$; power analysis 82.3%; Fig. 4B), HMT ($p = 0.010$; power analysis 98.5%; Fig. 4E), GFAP ($p = 0.002$; power analysis 100%; Fig. 5B), VIM ($p = 0.01$; power analysis 98.1%; Fig. 5E), and PLP ($p = 0.016$; power analysis 84.4%; Fig. 5H) mRNA levels was found only in late-stage AD (Braak stages 5–6) female patients as compared with control females (Braak stages 0–2).

Moreover, both H_3R and HMT correlated positively with Braak stages in females ($n = 26$, $\rho = 0.462$, $p = 0.001$ and

$\rho = 0.421$, $p = 0.003$ respectively), but not in males ($n = 23$, H_3R $\rho = 0.268$, $p = 0.229$ and HMT $\rho = 0.204$, $p = 0.350$).

4. Discussion

The present study demonstrates region-specific and sex-dependent changes in the human neuronal histamine system in AD. AD patients all showed a significant loss of the characteristic TMN neurons in all 3 subareas of the TMN. On the other hand, HDC mRNA expression, a marker for neuronal histamine production, was found only to diminish significantly in the central part of this nucleus (mTMN) in AD patients. The PFC, which is 1 of the major projection areas of histamine produced in the TMN (Haas et al., 2008), is affected relatively late in the course of AD (Braak and Braak, 1991). Only in females did we find a significantly increased H_3R , HMT, GFAP, VIM, and PLP mRNA expression in the PFC. Our findings indicate that the histaminergic system related to the PFC is especially affected in female AD patients. Moreover, although HMT mRNA levels were found to be positively correlated with GFAP

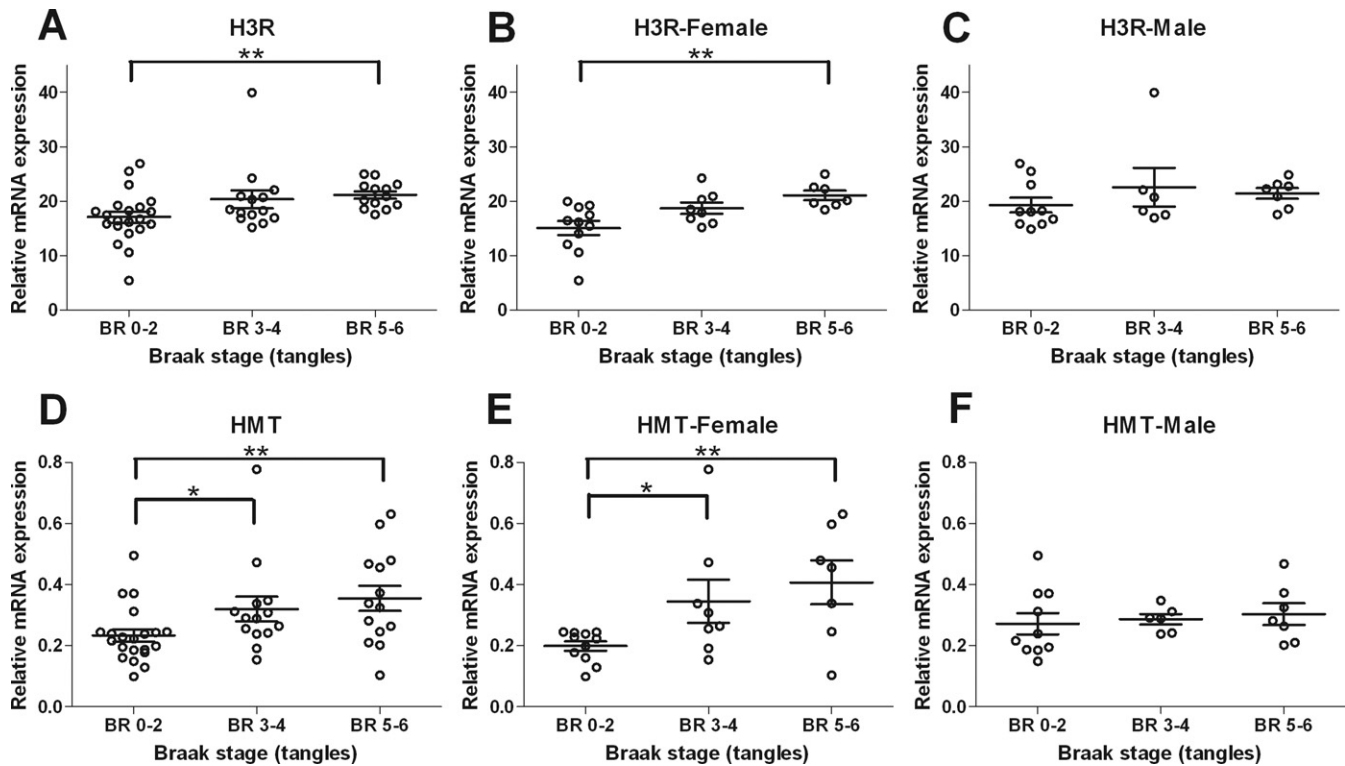


Fig. 4. The transcript level changes of histamine receptor-3 (H₃R) and the enzyme involved in histamine breakdown, histamine methyltransferase (HMT) in Alzheimer's disease (AD) prefrontal cortex (PFC). Results of quantitative polymerase chain reaction (qPCR) are shown as relative messenger (m) RNA expression for each gene normalized to the reference genes as described in Methods. Braak stage is indicated as BR followed by the number (0–6). Gene expression of (A) H₃R, and (D) HMT was significantly increased in end stage AD (BR 5–6; ** $p < 0.01$) compared with controls and preclinical stages: BR 0–2. (B) H₃R-mRNA expression was increased in BR 5–6 (** $p < 0.01$) only in females, not in males (C). (E) HMT mRNA expression was upregulated in females in BR 3–4 (* $p < 0.05$) and BR 5–6 (** $p < 0.01$). (F) In male subjects, HMT mRNA expression was unchanged in all stages.

mRNA, both in controls and AD patients, HMT mRNA was found exclusively in neurons in the human PFC.

4.1. Alteration in the TMN in AD

The total TMN neuron numbers of control subjects were quite comparable to those reported in a previous study (Airaksinen et al., 1991a). A novel observation is that the HDC mRNA production in the TMN was higher in control females than in males. Various sex differences have already been observed in this system. In human control subjects, ER α and β were expressed both in the cytoplasm and in the nucleus in a sex-dependent manner in the TMN (Kruijver et al., 2002, 2003). In view of the heterogeneous nature of the TMN (Giannoni et al., 2009; Sergeeva et al., 2002), we subdivided the TMN arbitrarily into 3 equal-length parts. The proportion of TMN neuronal loss in AD found in the present study (57%) is comparable with a previous study, which reported a 51% reduction of TMN cells in a smaller sample of patients, whereas only the rTMN and mTMN neurons were counted (Nakamura et al., 1993). It should be noted, however, that we do not know whether these neurons are actually dead and gone, or whether the atrophy renders the cells unrecognizable as typical TMN neurons. Because we only counted the typical, large TMN neurons that contain a clear nucleolus, the results of

cell counting may be interfered with significance by cellular atrophy. It is remarkable that the significant loss of large TMN neurons in AD patients is not accompanied by a significantly diminished HDC mRNA expression, which indicates that in AD the remaining TMN neurons are activated to compensate for the loss of active TMN neurons by enhanced histamine production. The slight (24%), nonsignificant decrease of HDC mRNA expression in the entire TMN of AD patients found in the present study is in agreement with the previous finding of a slightly lower level of the histamine metabolite tele-methyl-histamine (22%) in the cerebral spinal fluid of AD patients (Motawaj et al., 2010).

The TMN is known to be affected in early stage AD (Braak stage 3) by neurofibrillary pretangles as stained, e.g., by Alz-50, and by classic intraneuronal neurofibrillary tangles (Nakamura et al., 1993; Swaab et al., 1992; van de Nes et al., 1998). Because globular extracellular neurofibrillary tangles are present in the TMN the tangles were proposed to be involved in the loss of histaminergic neurons in this area (Airaksinen et al., 1991a, 1991b; Swaab, 2003). As mentioned above, the significant loss of large TMN neurons in AD patients is, however, largely compensated for as far as HDC mRNA expression is concerned. A similar compensation has been reported in the locus coeruleus, where the

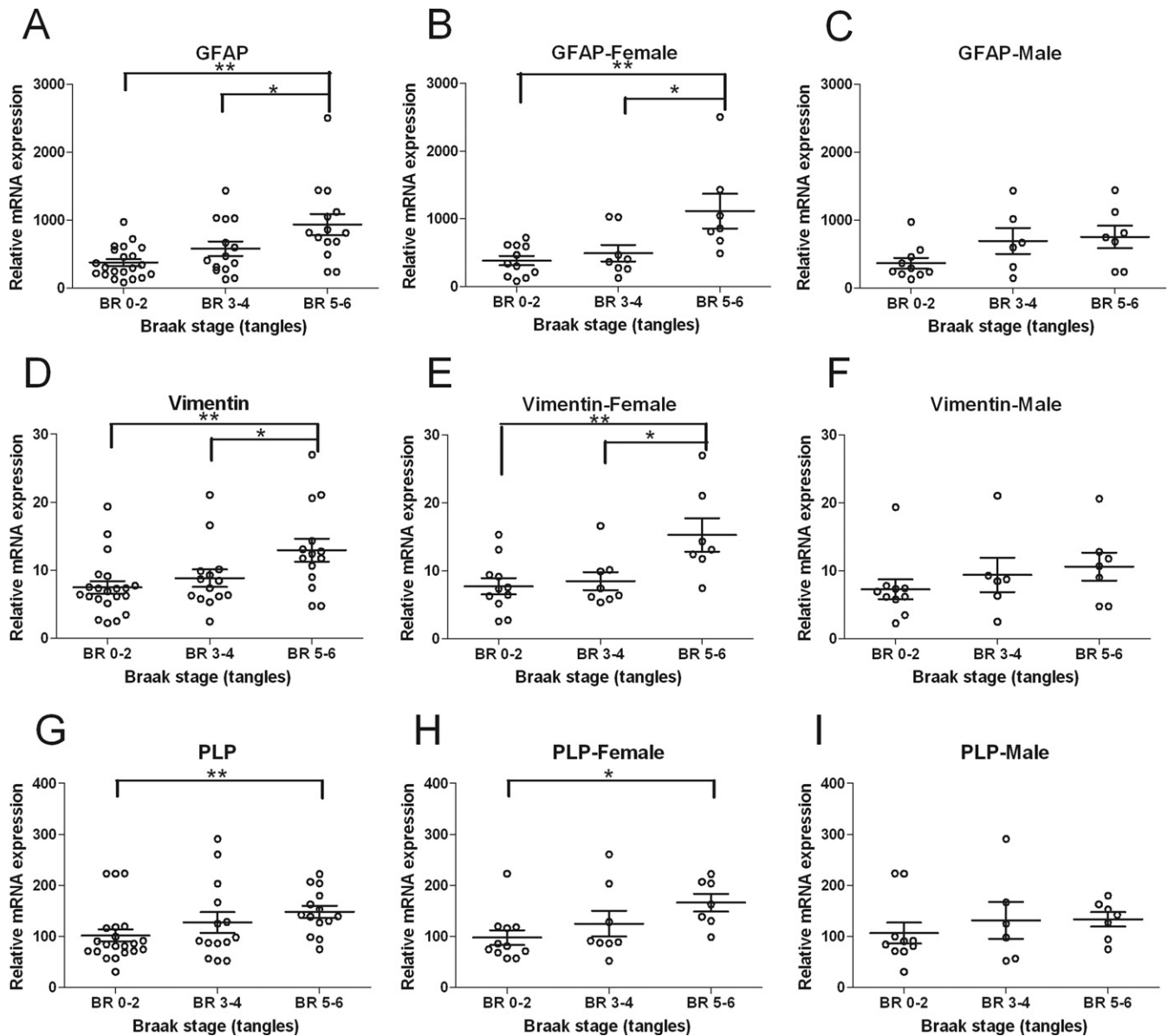


Fig. 5. The transcript level changes of glial fibrillary acidic protein (GFAP), vimentin, and proteolipid protein (PLP) in Alzheimer's disease (AD) prefrontal cortex (PFC). Results of quantitative polymerase chain reaction (qPCR) are shown as relative messenger (m) RNA expression for each gene normalized to the reference genes as described in Methods. Braak stage is indicated as BR followed by the number (0–6). Gene expression of (A) GFAP, (D) vimentin, (G) PLP was significantly increased in end stage AD (BR 5–6; ** $p < 0.01$) compared with controls and preclinical stages: BR 0–2. (B) GFAP mRNA (E) vimentin mRNA expression was increased in BR 5–6 compared with BR 0–2 (** $p < 0.01$), and preclinical stages BR 3–4 compared with BR 5–6 (* $p < 0.05$). The differences were only present in females, not in males (C) and (F). (H) PLP mRNA expression was upregulated in females in BR 5–6 (* $p < 0.05$) and not in males (I).

small proportion of remaining noradrenergic neurons are hyperactive in AD (Hoogendijk et al., 1999; Raskind et al., 1999; Szot et al., 2006). The alternative possibility, i.e., that the preservation of HDC mRNA could reflect preserved synthesis in atrophic neurons is less likely, given that generally many proteins are downregulated in atrophic neurons (Salehi et al., 1994).

The compensatory activation of histamine production was found to be complete in the rTMN and cTMN, while a significant reduction of HDC mRNA expression was found in mTMN (Fig. 4B). It is interesting to note that our group

previously observed a smaller Golgi apparatus size of TMN neurons, a marker for lower TMN neuronal metabolic activity, in the mTMN of AD patients (Salehi et al., 1995). The mTMN represents the largest proportion of both TMN neurons and HDC mRNA expression (Fig. 3).

4.2. Alterations in the PFC histaminergic system and glia cells

Our current finding of a higher expression of the histamine catabolic enzyme, HMT, and of the histamine (H_3

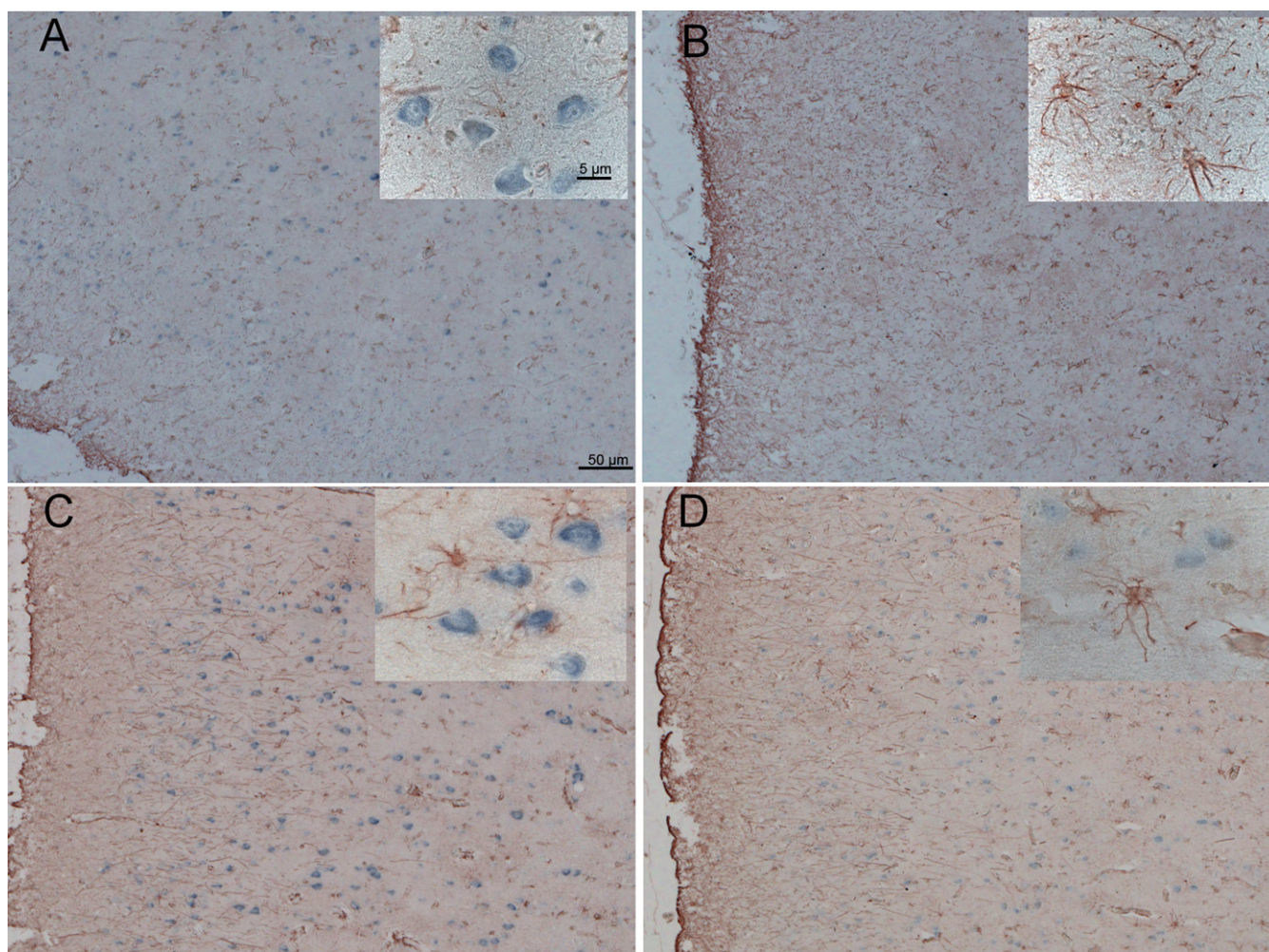


Fig. 6. Glial fibrillary acidic protein (GFAP) immunocytochemistry and histamine methyltransferase (HMT) messenger (m) RNA in situ hybridization in the human prefrontal cortex (PFC). (A) Specific HMT mRNA in situ hybridization signal (blue) was observed after hybridization with HMT antisense probe in the PFC Braak stage 6—Alzheimer's disease patient (Netherlands Brain Bank [NBB] # 98-147) with GFAP (red) double staining. Inset shows detail of the HMT-mRNA neuronal staining and astroglial GFAP staining. (B) Absence of blue staining after hybridization with sense probe in adjacent section from same subjects. Inset shows detail about the absence of HMT mRNA neuronal staining and positive astroglial staining. (C) and (D) Representative double staining in a control (NBB # 98-101) and a Braak stage 3 subject (NBB # 98-189), and insets show detailed HMT mRNA neuronal staining and GFAP astroglial cell staining, respectively. Scale bar for A–D = 50 μ m; scale bar for insets = 5 μ m.

receptor of female AD patients indicates a higher activity of, and sensitivity for, the histaminergic system in the PFC in female AD patients. It should be noted that we found HMT mRNA expression to be upregulated already in Braak stage 3–4, the same stage where neurofibrillary tangles in the TMN were first observed (Braak et al., 1993). HMT mRNA expression levels stayed higher in female end-stage AD patients compared with female controls. In spite of the positive correlation in the PFC between HMT mRNA and the astrocyte marker, both in the controls and in AD patients, we did not find colocalization of HMT mRNA and GFAP, while astrocytes were proposed to be the main inactivation site of histamine in animal brains (Husztai et al., 1990; Nishibori et al., 2000; Rafałowska et al., 1987). Our qPCR data also confirm the observation that astrocytes are activated in the PFC in the course of

AD (Coulson et al., 2010; Simpson et al., 2010). However, to our knowledge, we are the first to show that glia activation shown by GFAP, VIM, and PLP mRNA expression in the AD cerebral cortex only occurs in females.

In contrast to the increased HMT mRNA expression that we observed, Schneider et al. reported a significant decrease of HMT enzyme activity in AD PFC (Schneider et al., 1997). There are at least 2 possible explanations for these apparently contradictory results: (1) protein expression and posttranslational modifications can be disturbed, as was shown for other proteins in the AD brain (Butterfield et al., 2003); (2) histamine degradation requires the coenzyme S-adenosyl-methionine as methyl donor (Haas et al., 2008), while this compound is diminished in AD (reviewed in Shea and Chan, 2008).

We found also that H₃R mRNA expression was increased in the PFC in female AD patients. The main H₃R mRNA assayed in our qPCR study is most probably the heteroreceptor H₃R, produced by cortical neurons (Arrang et al., 2007), although a potential additional source of H₃R as an autoreceptor localized on the fibers of the histaminergic projecting neurons from the TMN, i.e., on the presynaptic membrane (Haas et al., 2008), cannot be entirely excluded. As a heteroreceptor, the activation of H₃R could at least partly account for the reported diminished release of several neurotransmitters in PFC, such as noradrenaline (Schlicker et al., 1999), gamma amino butyric acid (GABA) (Jang et al., 2001) and acetylcholine (Blandina et al., 1996). A deficiency of these neurotransmitters has indeed been reported in the PFC in AD (Bierer et al., 1995; Lanari et al., 2006), but the contribution of the histaminergic system to these changes has yet to be established. Interestingly, sex differences in relation to AD were also observed in the cholinergic system. The nucleus basalis of Meynert (NBM) is the major source of acetylcholine for the cortex (Mesulam et al., 1983). Female AD patients matched for age showed more severe early cytoskeletal alterations (Salehi et al., 1998) in the nucleus basalis of Meynert. Our data, together with previous findings, seem to offer a neurochemical basis for the observation that female AD patients show more pronounced cognitive deficits during the course of their disease (Henderson, 1997). Our present data may also provide a rationale for the use of H₃R antagonists, in particular in female AD patients, because these compounds increase the release of histamine, acetylcholine, noradrenaline, and dopamine, and may in this way modulate cognitive processes (Arrang et al., 2007). Their potential benefit for cognition has already been shown in preclinical trials (Brioni et al., 2010). However, so far no special attention has been paid to any such sex differences.

In our study H₁R mRNA expression in the medial frontal gyrus of the PFC was unchanged throughout the different Braak stages. This finding is in agreement with the observation that H₁R binding as measured by positron emission tomography (PET) was unaltered in the medial frontal gyrus (Brodman area 46) in AD patients (Higuchi et al., 2000). Interestingly, H₁R binding was decreased in the rest of the PFC, such as the superior frontal gyrus (Brodman area 9) (Higuchi et al., 2000). In accordance with our current data that the expression level of H₂R mRNA was unaltered in AD, Perry et al. (1998) also found H₂R binding to be unchanged in AD PFC.

The novel histamine receptor H₄R was recently found to be functionally expressed in the human cortex (Connelly et al., 2009). We report here for the first time that the H₄R mRNA tended to be higher in the PFC in AD than in controls. Further work is required to determine its localization and the mechanism underlying this change.

Some limitations of the present study should be mentioned: (1) the lack of suitable antibodies prevented immu-

nocytochemistry for the localization of H₁₋₄R or HMT in the PFC; (2) larger samples including different sexes are warranted for future investigations; (3) although the histaminergic alterations were measured both in the production site (TMN) and the projection site (PFC), material of both sites was only available for a few cases, which prohibited correlation analyses of the changes in the 2 areas.

In summary, these data provide insight into alterations at the production site, the TMN, and at a projection site, the PFC, of the neuronal histaminergic system in AD. The severe loss of TMN neurons in all 3 TMN subregions in late AD stages is largely compensated for by the histamine production as indicated by the overall unaltered HDC mRNA expression. However, HDC mRNA expression was diminished in the mTMN of AD patients. In addition, increased H₃R and HMT mRNA expression was found in the PFC in AD patients, but only in females. Moreover, a significant positive correlation was observed in females between the H₃R mRNA and HMT mRNA levels on the one hand and AD Braak-stages on the other. In spite of the positive correlation between HMT mRNA and the astrocyte marker in the controls and in AD patients, there was no colocalization of HMT mRNA and GFAP in astrocytes in the human PFC. The neuronal histaminergic alterations may be related to cognitive decline, especially in female AD patients. Furthermore, this study provides a rationale for H₃R inverse agonists as a potential AD treatment in the early stages of AD, especially in female patients.

Disclosure statement

The authors disclose no conflicts of interest.

The appropriate approval was obtained and the appropriate procedures followed with regard to the human material used in the current report. All the patients are donors from the Netherlands Brain Bank. Written informed consent for brain autopsy and for the use of brain tissue and clinical records for research purposes was provided by the patients' next of kin before subjects entered the study.

Acknowledgements

This work was supported by the China Scholarship Council for State Scholarship Fund (Grant number [2007] 3020) to L.S. A.-M.B. and D.F.S. were supported by the China Exchange Programme of the Royal Netherlands Academy of Arts and Sciences (KNAW Project 10CDP037). Dr. Ai-Min Bao was supported by the Fundamental Research Funds for the Central Universities China.

The authors are grateful to the Netherlands Brain Bank (Director Dr. Inge Huitinga) for providing human brain material and clinical details, and to Arja Sluiter for technical support. The authors also gratefully acknowledge Willem Kamphuis, Sabina Luchetti, and Wilma Verweij for com-

ments and corrections of the manuscript, and Mr. Bart Fisser and Mr. Ton Put for their technical assistance.

Appendix A. Supplementary data

Supplementary data associated with this article can be found, in the online version, at [doi:10.1016/j.neurobiolaging.2011.12.026](https://doi.org/10.1016/j.neurobiolaging.2011.12.026).

References

- Airaksinen, M.S., Paetau, A., Paljarvi, L., Reinikainen, K., Riekkinen, P., Suomalainen, R., Pænula, P., 1991a. Histamine neurons in human hypothalamus: anatomy in normal and Alzheimer diseased brains. *Neuroscience* 44, 465–481.
- Airaksinen, M.S., Reinikainen, K., Riekkinen, P., Pænula, P., 1991b. Neurofibrillary tangles and histamine-containing neurons in Alzheimer hypothalamus. *Agents Actions* 33, 104–107.
- Arrang, J.M., Morisset, S., Gbahou, F., 2007. Constitutive activity of the histamine H3 receptor. *Trends Pharmacol. Sci.* 28, 350–357.
- Bancher, C., Jellinger, K., Lassmann, H., Fischer, P., Leblhuber, F., 1996. Correlations between mental state and quantitative neuropathology in the Vienna Longitudinal Study on Dementia. *Eur. Arch. Psychiatry Clin. Neurosci.* 246, 137–146.
- Bierer, L.M., Haroutunian, V., Gabriel, S., Knott, P.J., Carlin, L.S., Purohit, D.P., Perl, D.P., Schmeidler, J., Kanof, P., Davis, K.L., 1995. Neurochemical correlates of dementia severity in Alzheimer's disease: relative importance of the cholinergic deficits. *J. Neurochem.* 64, 749–760.
- Blandina, P., Giorgetti, M., Bartolini, L., Cecchi, M., Timmerman, H., Leurs, R., Pepeu, G., Giovannini, M.G., 1996. Inhibition of cortical acetylcholine release and cognitive performance by histamine H3 receptor activation in rats. *Br. J. Pharmacol.* 119, 1656–1664.
- Bossers, K., Wirz, K.T., Meerhoff, G.F., Essing, A.H., van Dongen, J.W., Houba, P., Kruse, C.G., Verhaagen, J., Swaab, D.F., 2010. Concerted changes in transcripts in the prefrontal cortex precede neuropathology in Alzheimer's disease. *Brain* 133, 3699–3723.
- Braak, H., Braak, E., 1991. Neuropathological staging of Alzheimer-related changes. *Acta Neuropathol.* 82, 239–259.
- Braak, H., Braak, E., Bohl, J., 1993. Staging of Alzheimer-related cortical destruction. *Eur. Neurol.* 33, 403–408.
- Brioni, J.D., Esbenshade, T.A., Garrison, T.R., Bitner, S.R., Cowart, M.D., 2010. Discovery of histamine H3 antagonists for the treatment of cognitive disorders and Alzheimer's disease. *J. Pharmacol. Exp. Ther.* 336, 38–46.
- Butterfield, D.A., Boyd-Kimball, D., Castegna, A., 2003. Proteomics in Alzheimer's disease: insights into potential mechanisms of neurodegeneration. *J. Neurochem.* 86, 1313–1327.
- Cacabelos, R., Yamatodani, A., Niigawa, H., Hariguchi, S., Tada, K., Nishimura, T., Wada, H., Brandeis, L., Pearson, J., 1989. Brain histamine in Alzheimer's disease. *Methods Find. Exp. Clin. Pharmacol.* 11, 353–360.
- Connelly, W.M., Shenton, F.C., Lethbridge, N., Leurs, R., Waldvogel, H.J., Faull, R.L., Lees, G., Chazot, P.L., 2009. The histamine H4 receptor is functionally expressed on neurons in the mammalian CNS. *Br. J. Pharmacol.* 157, 55–63.
- Coulson, D.T., Beyer, N., Quinn, J.G., Brockbank, S., Hellemans, J., Irvine, G.B., Ravid, R., Johnston, J.A., 2010. BACE1 mRNA Expression in Alzheimer's Disease Postmortem Brain Tissue. *J. Alzheimers Dis.* 22, 1111–1122.
- Dubelaar, E.J., Mufson, E.J., ter Meulen, W.G., Van Heerikhuizen, J.J., Verwer, R.W., Swaab, D.F., 2006. Increased metabolic activity in nucleus basalis of Meynert neurons in elderly individuals with mild cognitive impairment as indicated by the size of the Golgi apparatus. *J. Neuropathol. Exp. Neurol.* 65, 257–266.
- Duncan, I.D., Hammang, J.P., Trapp, B.D., 1987. Abnormal compact myelin in the myelin-deficient rat: absence of proteolipid protein correlates with a defect in the intraperiod line. *Proc. Natl. Acad. Sci. U. S. A.* 84, 6287–6291.
- Eng, L.F., Ghinikar, R.S., Lee, Y.L., 2000. Glial fibrillary acidic protein: GFAP-thirty-one years (1969–2000). *Neurochem. Res.* 25, 1439–1451.
- Fernández-Novoa, L., Cacabelos, R., 2001. Histamine function in brain disorders. *Behav. Brain Res.* 124, 213–233.
- Fleige, S., Pfaffl, M.W., 2006. RNA integrity and the effect on the real-time qRT-PCR performance. *Mol. Aspects Med.* 27, 126–139.
- Ghi, P., Orsetti, M., Gamalero, S.R., Ferretti, C., 1999. Sex differences in memory performance in the object recognition test. Possible role of histamine receptors. *Pharmacol. Biochem. Behav.* 64, 761–766.
- Giannoni, P., Passani, M.B., Nosi, D., Chazot, P.L., Shenton, F.C., Medhurst, A.D., Munari, L., Blandina, P., 2009. Heterogeneity of histaminergic neurons in the tuberomammillary nucleus of the rat. *Eur. J. Neurosci.* 29, 2363–2374.
- Haas, H.L., Sergeeva, O.A., Selbach, O., 2008. Histamine in the nervous system. *Physiol. Rev.* 88, 1183–1241.
- Henderson, V.W., 1997. Estrogen, cognition, and a woman's risk of Alzheimer's disease. *Am. J. Med.* 103, 11S–18S.
- Higuchi, M., Yanai, K., Okamura, N., Meguro, K., Arai, H., Itoh, M., Iwata, R., Ido, T., Watanabe, T., Sasaki, H., 2000. Histamine H(1) receptors in patients with Alzheimer's disease assessed by positron emission tomography. *Neuroscience* 99, 721–729.
- Hoogendijk, W.J., Feenstra, M.G., Botterblom, M.H., Gilhuis, J., Sommer, I.E., Kamphorst, W., Eikelenboom, P., Swaab, D.F., 1999. Increased activity of surviving locus ceruleus neurons in Alzheimer's disease. *Ann. Neurol.* 45, 82–91.
- Husztai, Z., Magyar, K., Kálmán, M., 1990. Contribution of glial cells to histamine inactivation. *Agents Actions* 30, 237–239.
- Husztai, Z., Prast, H., Tran, M.H., Fischer, H., Philippu, A., 1998. Glial cells participate in histamine inactivation in vivo. *Naunyn Schmiedeberg's Arch. Pharmacol.* 357, 49–53.
- Jang, I.S., Rhee, J.S., Watanabe, T., Akaike, N., Akaike, N., 2001. Histaminergic modulation of GABAergic transmission in rat ventromedial hypothalamic neurones. *J. Physiol.* 534, 791–803.
- Jing, R., Wilhelmsson, U., Goodwill, W., Li, L., Pan, Y., Pekny, M., Skalli, O., 2007. Synemin is expressed in reactive astrocytes in neurotrauma and interacts differentially with vimentin and GFAP intermediate filament networks. *J. Cell Sci.* 120, 1267–1277.
- Koning, N., Bö, L., Hoek, R.M., Huitinga, I., 2007. Downregulation of macrophage inhibitory molecules in multiple sclerosis lesions. *Ann. Neurol.* 62, 504–514.
- Kruijver, F.P., Balesar, R., Espila, A.M., Unmehopa, U.A., Swaab, D.F., 2002. Estrogen receptor-alpha distribution in the human hypothalamus in relation to sex and endocrine status. *J. Comp. Neurol.* 454, 115–139.
- Kruijver, F.P., Balesar, R., Espila, A.M., Unmehopa, U.A., Swaab, D.F., 2003. Estrogen-receptor-beta distribution in the human hypothalamus: similarities and differences with ER alpha distribution. *J. Comp. Neurol.* 466, 251–277.
- Lanari, A., Amenta, F., Silvestrelli, G., Tomassoni, D., Parnetti, L., 2006. Neurotransmitter deficits in behavioural and psychological symptoms of Alzheimer's disease. *Mech. Ageing Dev.* 127, 158–165.
- Lees, M.B., Samiullah, M., Laursen, R.A., 1984. Structural analogies between myelin basic protein and proteolipid. *Prog. Clin. Biol. Res.* 146, 257–264.
- Liu, C.Q., Shan, L., Balesar, R., Luchetti, S., Van Heerikhuizen, J.J., Luo, J.H., Swaab, D.F., Bao, A.M., 2010. A quantitative in situ hybridization protocol for formalin-fixed paraffin-embedded archival post-mortem human brain tissue. *Methods* 52, 359–366.
- Luchetti, S., Bossers, K., Van de Bilt, S., Agrapart, V., Morales, R.R., Frajese, G.V., Swaab, D.F., 2011. Neurosteroid biosynthetic pathways changes in prefrontal cortex in Alzheimer's disease. *Neurobiol. Aging* 32, 1964–1976.

- Martorana, A., Esposito, Z., Koch, G., 2011. Beyond the cholinergic hypothesis: do current drugs work in Alzheimer's disease? *CNS Neurosci. Ther.* 16, 235–245.
- Mazurkiewicz-Kwilecki, I.M., Nsonwah, S., 1989. Changes in the regional brain histamine and histidine levels in postmortem brains of Alzheimer patients. *Can. J. Physiol. Pharmacol.* 67, 75–78.
- Mesulam, M.M., Mufson, E.J., Levey, A.I., Wainer, B.H., 1983. Cholinergic innervation of cortex by the basal forebrain: cytochemistry and cortical connections of the septal area, diagonal band nuclei, nucleus basalis (substantia innominata), and hypothalamus in the rhesus monkey. *J. Comp. Neurol.* 214, 170–197.
- Motawaj, M., Peoc'h, K., Callebert, J., Arrang, J.M., 2010. CSF Levels of the Histamine Metabolite *tele*-Methylhistamine are only Slightly Decreased in Alzheimer's Disease. *J. Alzheimers Dis.* 22, 861–871.
- Nakamura, S., Takemura, M., Ohnishi, K., Suenaga, T., Nishimura, M., Akiguchi, I., Kimura, J., Kimura, T., 1993. Loss of large neurons and occurrence of neurofibrillary tangles in the tuberomammillary nucleus of patients with Alzheimer's disease. *Neurosci. Lett.* 151, 196–199.
- Nishibori, M., Tahara, A., Sawada, K., Sakiyama, J., Nakaya, N., Saeki, K., 2000. Neuronal and vascular localization of histamine *N*-methyltransferase in the bovine central nervous system. *Eur. J. Neurosci.* 12, 415–424.
- Panula, P., Rinne, J., Kuokkanen, K., Eriksson, K.S., Sallmen, T., Kalimo, H., Relja, M., 1998. Neuronal histamine deficit in Alzheimer's disease. *Neuroscience* 82, 993–997.
- Panula, P., Yang, H.Y., Costa, E., 1984. Histamine-Containing Neurons in the Rat Hypothalamus. *Proc. Natl. Acad. Sci. U. S. A.* 81, 2572–2576.
- Pekny, M., Pekna, M., 2004. Astrocyte intermediate filaments in CNS pathologies and regeneration. *J. Pathol.* 204, 428–437.
- Perry, E., Court, J., Goodchild, R., Griffiths, M., Jaros, E., Johnson, M., Lloyd, S., Piggott, M., Spurdin, D., Ballard, C., McKeith, I., Perry, R., 1998. Clinical neurochemistry: developments in dementia research based on brain bank material. *J. Neural Transm.* 105, 915–933.
- Prell, G.D., Khandelwal, J.K., Burns, R.S., LeWitt, P.A., Green, J.P., 1988. Elevated levels of histamine metabolites in cerebrospinal fluid of aging, healthy humans. *Compr Gerontol [A]* 2, 114–119.
- Prell, G.D., Khandelwal, J.K., Burns, R.S., LeWitt, P.A., Green, J.P., 1990. Influence of age and gender on the levels of histamine metabolites and *pro*-methylimidazoleacetic acid in human cerebrospinal fluid. *Arch. Gerontol. Geriatr.* 11, 85–95.
- Rafałowska, U., Waśkiewicz, J., Albrecht, J., 1987. Is neurotransmitter histamine predominantly inactivated in astrocytes? *Neurosci. Lett.* 80, 106–110.
- Raskind, M.A., Peskind, E.R., Holmes, C., Goldstein, D.S., 1999. Patterns of cerebrospinal fluid catechols support increased central noradrenergic responsiveness in aging and Alzheimer's disease. *Biol. Psychiatry* 46, 756–765.
- Salehi, A., Gonzalez Martinez, V., Swaab, D.F., 1998. A sex difference and no effect of ApoE type on the amount of cytoskeletal alterations in the nucleus basalis of Meynert in Alzheimer's disease. *Neurobiol. Aging* 19, 505–510.
- Salehi, A., Heyn, S., Gonatas, N.K., Swaab, D.F., 1995. Decreased protein synthetic activity of the hypothalamic tuberomammillary nucleus in Alzheimer's disease as suggested by smaller Golgi apparatus. *Neurosci. Lett.* 193, 29–32.
- Salehi, A., Lucassen, P.J., Pool, C.W., Gonatas, N.K., Ravid, R., Swaab, D.F., 1994. Decreased neuronal activity in the nucleus basalis of Meynert in Alzheimer's disease as suggested by the size of the Golgi apparatus. *Neuroscience* 59, 871–880.
- Schlicker, E., Werthwein, S., Zentner, J., 1999. Histamine H3 receptor-mediated inhibition of noradrenaline release in the human brain. *Fundam. Clin. Pharmacol.* 13, 120–122.
- Schneider, C., Risser, D., Kirchner, L., Kitzmüller, E., Cairns, N., Prast, H., Singewald, N., Lubec, G., 1997. Similar deficits of central histaminergic system in patients with Down syndrome and Alzheimer disease. *Neurosci. Lett.* 222, 183–186.
- Sergeeva, O.A., Eriksson, K.S., Sharonova, I.N., Vorobjev, V.S., Haas, H.L., 2002. GABA(A) receptor heterogeneity in histaminergic neurons. *Eur. J. Neurosci.* 16, 1472–1482.
- Shea, T.B., Chan, A., 2008. S-adenosyl methionine: a natural therapeutic agent effective against multiple hallmarks and risk factors associated with Alzheimer's disease. *J. Alzheimers Dis.* 13, 67–70.
- Simpson, J.E., Ince, P.G., Lace, G., Forster, G., Shaw, P.J., Matthews, F., Savva, G., Brayne, C., Wharton, S.B., MRC Cognitive Function and Ageing Neuropathology Study Group, 2010. Astrocyte phenotype in relation to Alzheimer-type pathology in the ageing brain. *Neurobiol. Aging* 31, 578–590.
- Swaab, D.F., 2003. *The Human Hypothalamus: Basic and Clinical Aspects. Part 1: Nuclei of the Human Hypothalamus.* Elsevier, Amsterdam.
- Swaab, D.F., Grundke-Iqbal, I., Iqbal, K., Kremer, H.P., Ravid, R., van de Nes, J.A., 1992. Tau and ubiquitin in the human hypothalamus in aging and Alzheimer's disease. *Brain Res.* 590, 239–249.
- Szot, P., White, S.S., Greenup, J.L., Leverenz, J.B., Peskind, E.R., Raskind, M.A., 2006. Compensatory changes in the noradrenergic nervous system in the locus ceruleus and hippocampus of postmortem subjects with Alzheimer's disease and dementia with Lewy bodies. *J. Neurosci.* 26, 467–478.
- van de Nes, J.A., Kamphorst, W., Ravid, R., Swaab, D.F., 1998. Comparison of beta-protein/A4 deposits and Alz-50-stained cytoskeletal changes in the hypothalamus and adjoining areas of Alzheimer's disease patients: amorphous plaques and cytoskeletal changes occur independently. *Acta Neuropathol.* 96, 129–138.
- Vandesompele, J., De Preter, K., Pattyn, F., Poppe, B., Van Roy, N., De Paepe, A., Speleman, F., 2002. Accurate normalization of real-time quantitative RT-PCR data by geometric averaging of multiple internal control genes. *Genome Biol.* 3, RESEARCH0034.
- Verwer, R.W., Raber-Durlacher, J.E., 1993. Efficient and unbiased estimation of volume and area of tissue components and cell number in gingival biopsies. *J. Periodontol. Res.* 28, 313–323.
- Yanai, K., Tashiro, M., 2007. The physiological and pathophysiological roles of neuronal histamine: an insight from human positron emission tomography studies. *Pharmacol. Ther.* 113, 1–15.